

Experimental studies of laser focusing conditions on electron acceleration in underdense plasma interactions

A G R Thomas, C D Murphy*, S P D Mangles, Z Najmudin, W Rozmus[†], A E Dangor, K Krushelnick

Blackett Laboratory, Imperial College London, SW7 2BZ, UK

P S Foster, P A Norreys, E J Divall, C J Hooker, A J Langley, J M Smith, J L Collier

Central Laser Facility, CCLRC Rutherford Appleton Laboratory, Chilton, Didcot, Oxon., OX11 0QX, UK

J G Gallacher, D A Jaroszynski

Department of Physics, University of Strathclyde, Glasgow, G4 0NG, UK

Main contact email address: alec.thomas@imperial.ac.uk

*also based at the Central Laser Facility

[†] Permanent address: Department of Physics, University of Alberta, Edmonton, Canada

Introduction

The idea to use lasers propagating through underdense plasma to accelerate particles to relativistic energies in plasma was first suggested over 20 years ago¹. Recent experiments² have demonstrated the feasibility of the production of relativistic electron beams with high energies, low energy spread and low emittance. Of the numerous laser based schemes for plasma accelerators³, only the laser wakefield (LWF) acceleration scheme has so far been able to produce highly collimated, monoenergetic electron beams². The LWF accelerator consists of a high intensity laser pulse propagating through a plasma, such that the laser pulse length is shorter than the relativistic plasma wavelength ($c\tau < \lambda_p = 2\pi c/\omega_p$). The energy density of the laser pulse is sufficient to displace—through $\mathbf{v} \times \mathbf{B}$ and nonlinear forces collectively known as the ponderomotive force—the electrons in its path. The electrons then oscillate due to the resulting space charge separation between the electrons and ions, which due to their mass can be considered stationary.

The phase velocity of the electron plasma wave fronts is the group velocity of the pulse in the plasma, given by $(1 - \omega_p^2/\omega^2)^{1/2}c$, where ω is the laser frequency, and ω_p the plasma frequency. Electrons with oscillation velocities exceeding this phase speed can remain in the accelerating phase of the longitudinal electric field. These electrons can reach energies determined by the electric field in the plasma wave and the length over which the acceleration takes place. The maximum electric field is, in the cold one-dimensional limit, $E_{\max} = [2(\gamma_{\text{ph}} - 1)]^{1/2} \cdot m_e c \omega_p / e$ ⁴, where $\gamma_{\text{ph}} = (1 - \beta_{\text{ph}}^2)^{-1/2}$ and $\beta_{\text{ph}}c$ is the phase velocity of the plasma wave.

In higher dimensions the physics is more complicated, and as yet there is no fully 3D nonlinear analytic model to describe interactions. However, it is suggested⁵ that multidimensional effects lower the wavebreaking threshold, and in essence the threshold is a function of the laser pulse shape. Ideally the pulse wants to be temporally short and larger radially (close to $2\pi c/\omega_p$ ⁶).

We report on an experiment to directly compare the effect of different initial pulse shapes on the electron beam characteristics, and show that the focusing geometry is critical particularly in determining the electron spectrum.

Experiment

The experiments were carried out on the Ti:Sapphire Astra laser at the Rutherford Appleton Laboratory, which provided pulses of energy up to $EL = 600$ mJ, pulse length $\tau = 40(\pm 5)$ fs FWHM and centre wavelength $\lambda_0 = 790$ nm. The laser was focused with either $f/3$ or $f/16$ off axis parabolic mirrors, where the f -number refers to the ratio of focal length to initial beam diameter. The measured beam waists at focus were $5 \mu\text{m}$ and $25 \mu\text{m}$ respectively, resulting in vacuum focused intensities of $3.5 \times 10^{19} \text{ Wcm}^{-2}$ and $2 \times 10^{18} \text{ Wcm}^{-2}$ corresponding to normalized vector potentials $a_0 = eA/m_e c$ of 4 and 1. The laser pulses were focused onto the front edge of a 2 mm diameter conical helium gas jet. This provided initial electron densities of $3 \times 10^{18} \text{ cm}^{-3} < n_e < 5 \times 10^{19} \text{ cm}^{-3}$.

The light transmitted through the interaction was measured after reflection by a glass plate, which served to attenuate the intensity and limit spectral modifications caused by the window of the target chamber. Light within an $f/5$ cone was collimated and re-imaged to the slit of a 150 lines/mm grating spectrometer. The spectrum was recorded on a 16 bit CCD camera, and corrected for spectral sensitivity. The resulting 2D image was spectrally dispersed in one direction, but profile information was retained in the other direction. The glass plate had a 1 cm diameter hole allowing uninhibited passage of electrons to an electron spectrometer. This means that light was not collected in a central region of $f/25$.

The energy spectrum of the accelerated electrons was obtained using a magnetic spectrometer using image plate detectors. Image plates have excellent dynamic range and resolution, and allow single shot acquisition of the full spectrum⁷. Light scattered from the interaction was re-imaged orthogonally to the beam axis, both perpendicular (top view) and parallel (side

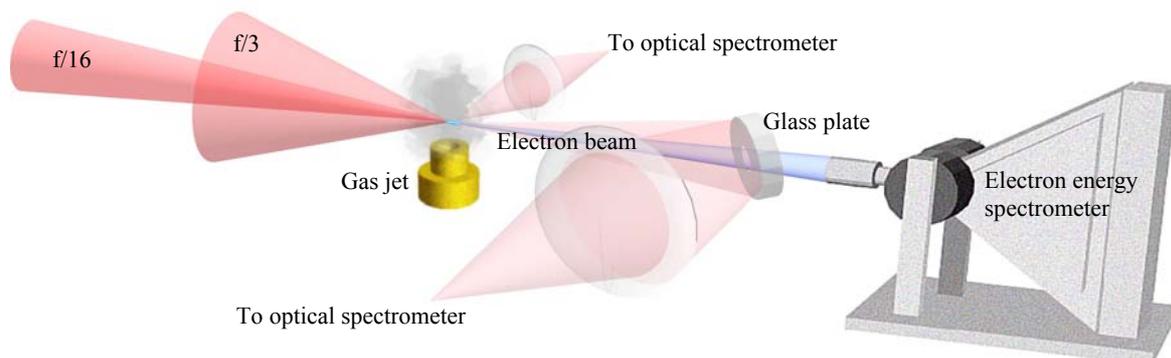


Figure 1. Experimental setup.

view) to the laser polarization plane. Measurements of the electron beam profile were made using stacks of radiochromic film interleaved with copper pieces of known thickness placed on the laser axis after focus.

Experimental Results

Figure 2 shows typical Thomson scattering images from the experiment. The extent of the visible channel is shorter for the $f/3$ ($<80\ \mu\text{m}$) interaction than the $f/16$ ($\sim 700\ \mu\text{m}$). In fact the extent of scattering for the $f/16$ can be shorter than $700\ \mu\text{m}$ under certain conditions, down to $200\ \mu\text{m}$ or less, and also longer, extending to the length of the gas jet. The exact nature of the relationship between the observed channel length and laser or electron beam characteristics has yet to be determined.

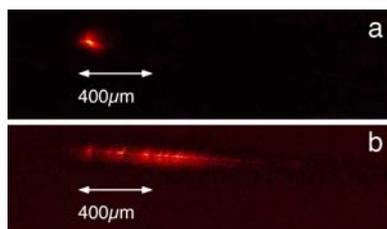


Figure 2. Thomson scattered light from the interaction imaged at 90° to the laser polarization and the beam axis for typical shots at $n_e = 2 \times 10^{19}\ \text{cm}^{-3}$ for a) $f/3$ and b) $f/16$.

However the $f/3$ interaction length is without exception restricted to less than $100\ \mu\text{m}$. This can be simply attributed to the differences in vacuum Rayleigh length, although due to self-focusing of the pulse it may be more complicated in reality⁶.

The angular divergence of the electrons produced by the $f/3$ was $\sim 15^\circ$. In the case of the $f/16$, the divergence of the high ($>1\ \text{MeV}$) energy electrons for the $f/16$ is less than 1° . The energy of the electrons is calculated from their penetration through copper pieces. Analysis can show that the spreading of the beam as it propagates through the $1\ \text{mm}$ copper pieces corresponds to the spreading of a monoenergetic electron beam.

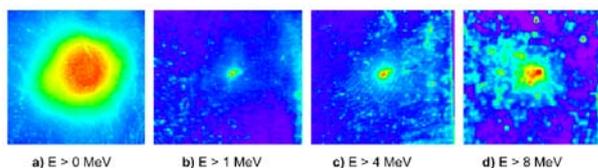


Figure 3. Radiochromic film images of the electron beam profile as it propagates through a) zero b) one c) two and d) four $1\ \text{mm}$ thickness copper pieces.

Electrons below $1\ \text{MeV}$ have a larger angular divergence, similar to that of the $f/3$. Fig. 3 shows radiochromic film from a copper stack indicating the divergence of the electrons produced by the $f/16$ parabola for different energies. The $f/3$ divergence is similar to the low energy ($<1\ \text{MeV}$) $f/16$ divergence and the tightly collimated electron beam does not appear.

The electron energy spectra at high density ($\omega_{pt} \gg 1$) are qualitatively similar for both $f/3$ and $f/16$ focusing. They are Maxwellian, like previous experiments in the “self-modulated” regime⁸) and can be characterized by an effective temperature. However, as the density is lowered so that $\omega_{pt} \rightarrow 2\pi$ – e.g. the pulse length approaches a relativistic plasma wavelength – the two focusing geometries behave in qualitatively different ways. In the case of the $f/3$, narrower energy spread features appear, but are superimposed on a background “dark current” of electrons that again takes a Maxwellian form. The short interaction length of the laser pulse presumably limits the acceleration length, but the very high intensity of the pulse still produces relativistic electrons. Figure 4 shows typical $f/3$ and $f/16$ spectra at lower density, as $\omega_{pt} \rightarrow 2\pi$.

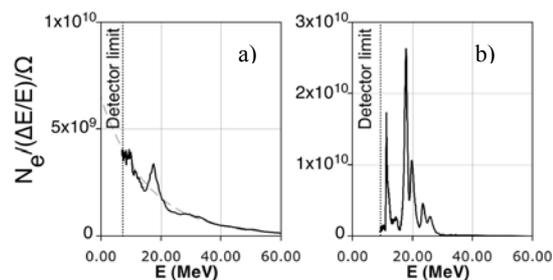


Figure 4. Electron energy spectra at a number density of $2 \times 10^{19}\ \text{cm}^{-3}$ for a) $f/3$ and b) $f/16$ focusing.

With $f/16$ focusing (Figure 4b), the background electron “dark current” appears to be suppressed, and instead the spectrum consists of multiple “spikes” or even a single monoenergetic peak. This is probably due to the increased interaction length, which allows a single, short electron bunch to be injected. The shortness of the bunch allows it to see a uniform electric field. This is combined with a “switching off” of electron injection due to beam loading, which is the interference of the electron bunch with the laser wakefield which prevents further injection. This monoenergetic peak cannot be characterized by a temperature, but by a peak energy and energy spread.

In summary, the characteristics of a laser wakefield accelerated electron beam are greatly improved by careful choice of the focusing geometry. Higher quality beams can be produced by choosing longer focal length geometries despite the lower intensities that result.

Acknowledgements

The authors acknowledge the support of UK EPSRC. The authors comprise a section of the Alpha-X collaboration and gratefully acknowledge the work of other collaborators. This work is supported by Research Councils UK.

References

1. T Tajima and J M Dawson, Phys. Rev. Lett. **43**, 267 (1979)
2. S P D Mangles *et al.*, Nature **431**, 535 (2004); C G R Geddes *et al.*, Nature **431**, 538 (2004); J Faure *et al.*, Nature **431**, 541 (2004); S Fritzler *et al.*, Phys. Rev. Lett. **92**, 16 (2004); S P D Mangles *et al.*, accepted, Phys. Rev. Lett. (2005); V. Malka *et al.*, Science **298**, 1596 (2002).
3. E Esarey *et al.*, IEEE Trans Plas Sci, **24(2)**:252-288. (1996)
4. A I Akhiezer and RV Polovin, Sov Phys JETP, **3**:696-705 (1956)
5. S V Bulanov *et al.*, Phys. Rev. Lett. **78**, 4205 (1997).
6. A G R Thomas *et al.*, to be submitted Phys. Rev. Lett.
7. Iwabuchi *et al.*, Jpn. J. Appl. Phys, **33**, 178 (1994).
8. P Sprangle *et al.*, Appl. Phys. Lett. **53**, 2146 (1988); N Andreev *et al.*, JETP Lett. **55**, 571 (1992).